J. COMBIN. MATH. COMBIN. COMPUT. 127b (2025) 7565--7578

Journal of Combinatorial Mathematics and Combinatorial Computing
www.combinatorialpress.com/jcmcc

Combinatorial Press

Research on automated human health management based on DNNAS algorithm

Ying Zhu[1], Zekun Chen[2], Maoquan Su[1,3,✉]

[1]. School of Management, Shandong Second Medical University, Weifang, Shandong, 261000, China

[2]. Administrative Office of the Dean, Weifang People's Hospital, Weifang, Shandong, 261000, China

[3]. The First Affiliated Hospital of Shandong Second Medical University (Weifang People's Hospital), Weifang, Shandong, 261000, China

ABSTRACT
A method for automatic recognition and anomaly detection of electrocardiogram signals based on deep neural network structure search has been proposed. Firstly, the raw ECG signals are converted into various image representations, including Gram angle field, recursive mapping, Markov transition field, etc., which enables the deep learning model to better handle these complex signal features. Meanwhile, this study utilizes convolutional neural networks for feature extraction and learns the complex relationships between features through fully connected layers. The results demonstrated that the improved method achieved a maximum accuracy of 98.5% and an average accuracy of 94.0% on the PhysioNet MIT-BIH dataset. Additionally, on the PTB dataset, the average recall rate of the improved method reached 98.4%, surpassing the performance of traditional neural networks and Canny algorithm. The experimental results indicate that the research method effectively optimizes the key patterns' recognition ability in electrocardiogram signals and has excellent performance in detection results. This study offers a more reliable tool for early diagnosis and health management of human health diseases.

Keywords: DNNAS, Gram corner field, Recursive graph, Markov transition field, CNN, Human health.

1. Introduction

The rapid changes in science and technology have provided strong support for the continuous development and progress of social economy and the leap in people's quality of life [1-2]. However, the pressure of study, life and work come one after another, students face high-intensity learning pressure, adults face the pressure of mortgage, car loan, work competition and socializing, etc., and the elderly face the pressure of the heart of the retirement caused by the difference between the pressure of the

✉ Corresponding author.
E-mail address: zhuyingflx@163.com (M. Su).

Received 20 February 2024; Revised 15 May 2024; Accepted 20 November 2024; Published Online 16 April 2025.
DOI: 10.61091/jcmcc127b-413

heart, people in a long-term high-pressure state will lead to the organism in the health and disease between the state of sub-health [3-6]. People in a long-term subhealthy state, often ignore the physical discomfort, if not timely and effective interventions or intervention methods are not appropriate, then people's physical condition will gradually from the subhealthy state to the development of disease state [7-10]. Sub-health has become the number one invisible killer threatening human health, and at the same time, it is also a hot topic of medical research now.

In this context, realizing the provision of all-round and full-cycle health services for the people requires the use of intelligent ways to scientifically, safely, and effectively escort the health management of the people [11-12]. Among them, exercise prescription is an important means for people to improve their poor living habits, as well as to effectively improve their current physical health status with the help of proper exercise and regular diet [13-15]. Exercise prescription is not only limited to exercise, but also involves various fields, medical, physical education, nutrition, etc [16]. However, there are not many organizations that can issue scientific and effective exercise prescriptions in China, which makes it more difficult for the people to obtain their own matching healthy exercise prescriptions, or some fitness organizations and rehabilitation medical institutions issue exercise prescriptions for a short period of time, which are not effective in the long term [17-20]. As the people cannot obtain exercise prescription quickly and effectively, this greatly restricts the people's scientific exercise and healthy exercise [21-22]. Therefore, in order to effectively meet the needs of the public in their daily life can easily obtain the correct scientific exercise prescription, improve the bad habits, healthy diet and scientific exercise, there is an urgent need for an intelligent, scientific and comprehensive health management system [23-26]. Using intelligent algorithms as an analytical tool to prescribe scientific exercise prescriptions based on the individual differences of each population can increase the health awareness of the population and improve their subhealth conditions [27-29].

ECG signals are often affected by noise and various interferences, which may result in degradation of the signal quality, thus affecting the accuracy of the identification. ECG signals from various patients may exhibit different characteristics, making it difficult to generalize the model. In addition, different types of diseases may exhibit similar features on ECG signals, which increases the difficulty of disease identification. To address these issues and improve the analysis accuracy of ECG signals, this study adopts Deep Neural Network Architecture Search (DNNAS) as the signal recognition model for ECG. The innovation of the model is that it can automatically search and optimize the neural network structure to find the most suitable network structure for ECG signal recognition, avoiding the tedious process of manual trial and error. The accuracy of recognition is improved by converting the ECG signals into different forms of image data and effectively extracting complex features from the signals using methods such as deep learning. DNNAS can utilize large-scale datasets to train and optimize the model for better adaptability and generalization, enabling it to recognize abnormal signals from different patients.

2. Theoretical Framework

This study selects CNN as the main method for ECG signal feature extraction in DCN. CNN is a powerful deep learning model. It can extract important features from images and other grid data through multilevel convolution and pooling operations, and performs well in areas such as computer vision.

This study mainly uses CNN to extract ECG signal features in DCN. CNN extracts important features of image and grid information through multilevel convolution and pooling and excels in areas such as computer vision. Average pooling in CNN reduces the size of the feature map by taking the average of a set of neighboring feature maps. The pooling process retains relatively smooth and important features appearing in localized regions by aggregating information from neighboring features. This is useful for overall feature extraction of ECG signals, facilitating the identification of critical EEG patterns, timely monitoring of human health changes, and promoting timely medical intervention. The expression of CNN is shown in formula (1)

$$\begin{cases} H_{out} = \{(H_{in} + 2P - F)/S\} + 1 \\ W_{out} = \{(W_{in} + 2P - F)/S\} + 1 \end{cases} \tag{1}$$

In formula (1), H_{out} and W_{out} are the height and width of the image. P is the image filling dimension, F is the convolution kernel size, and S is the movement step size. CNNs are effective in human health management for extracting features from ECG signals and early identification of abnormal patterns such as arrhythmias. The average pooling operation of CNN is shown in Figure 1.

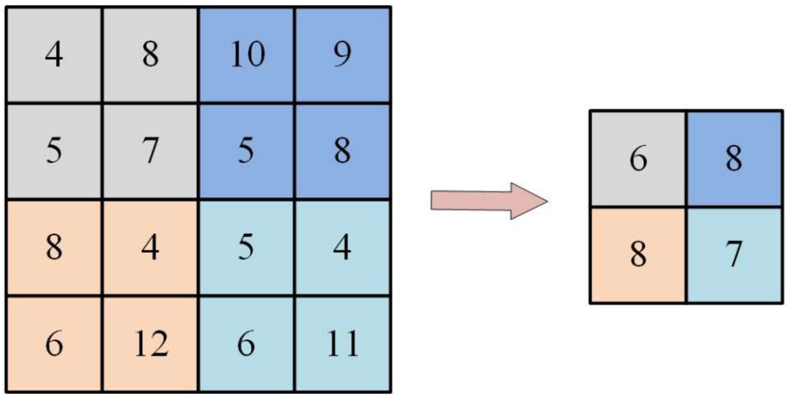

Fig. 1. Diagram of average pooling operation

In Figure 1, the average pooling operation is defined by defining a fixed-size pooling window in the input feature map, sliding the pooling window from the upper-left corner of the feature map, and moving it in certain steps. After each movement, the area under the window will be extracted for calculating the average value. The values within the area covered by each pooling window are calculated to obtain the average of these values. The Fully Connected Layer (FCL) in CNN flattens the feature maps from the convolutional and pooling layers, connecting all extracted features into a large vector. Through this approach, FCL is able to comprehensively analyze features and learn complex relationships between them.

3. Methodology

The research model converts raw ECG signals into different image data, including Graham's Corner Field (GCF), recursive maps, and Markov Transition Fields (MTF). The reason is that image data can visually display the characteristics of ECG signals. Different image transformations can extract and represent complex patterns and structures in signals, making deep learning models easier to train and recognize. Moreover, after image transformation, it is more suitable for processing using deep learning models.

3.1. Graham's corner field

GCF is a method of converting time series data into images, converting raw ECG signals into polarity encoding, and calculating the polar angle of each value. Second, the polar angles are utilized to construct a Gram matrix to compute the cosine similarity between each pair of points in the time series. Finally, the generated Gramian matrix can be further processed through methods such as color mapping and visualized as an image, as shown in Figure 2.

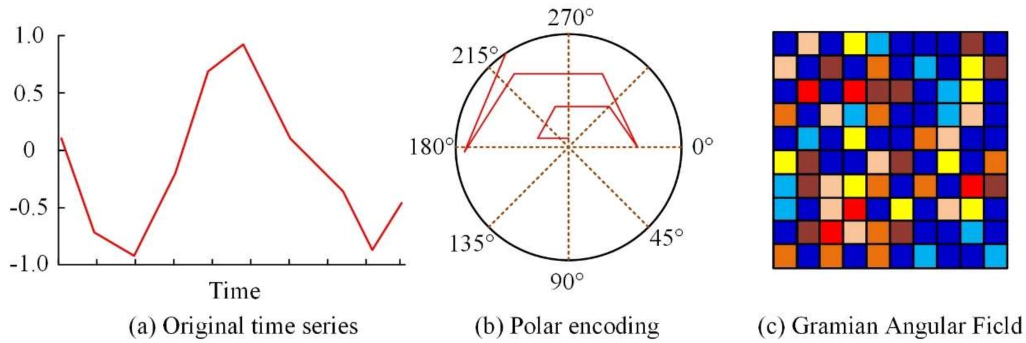

Fig. 2. Gram corner field diagram

In Figure 2, the original ECG signal is normalized to ensure that the data falls within the range of [-1,1]. Second, the normalized time series are converted to polar coding and the polar angle of each value is calculated. The conversion of polar field is shown in formula (2).

$$G(x^i)_{p,q} = \frac{1}{2}\cos(2\pi(x_p^i - x_q^i)/T) \tag{2}$$

In formula (2), G is the polar field, p and q are the time point, T is the period, and x^i is the time series. Deep learning models can obtain an intuitive representation of signals, effectively enhancing the recognition and analysis of pathological signals. Thereby, it can help physicians to make quick diagnostic and management decisions on human health. The calculation of Gram matrix G is shown in formula (3).

$$G_{i,j} = \frac{1}{z}\sum_{l=1}^{z} G(x_i^l)G(x_j^l) \tag{3}$$

In formula (3), z is the number of time periods. The constructed GCF can effectively capture the periodic characteristics and dynamic changes of human health data time series, reflecting the time-dependent nature of the signal.

3.2. Recursive graph

Recurrence diagrams are a visualization tool for analyzing dynamic systems and time-series data that reveal the dynamic nature, periodicity, and complexity of human health signals by describing how system states repeat over time. A recurrence diagram shows the reproduction relationship between any two time points in a time series, i.e., whether the states are similar at different time points. This study calculates ECG signals through recursive graphs, as shown in formula (4).

$$R = \alpha(\lambda - \|x_p - x_p\|) \tag{4}$$

In formula (4), R is the recursive graph, λ is the ECG signal threshold, and α is the heavy edge function. When analyzing ECG signals, potential abnormal activity or disease patterns can be identified.

3.3. Markov transition field

MTF is a technique for representing time series data in the form of images, aiming to capture dynamic features and patterns in a time series through transition relationships between states. The goal is to construct images describing the transition probabilities between the states of the human health time series, considering the states of the time series as pixels in the image, and then revealing the dynamics and underlying structure of the time series, as shown in Figure 3.

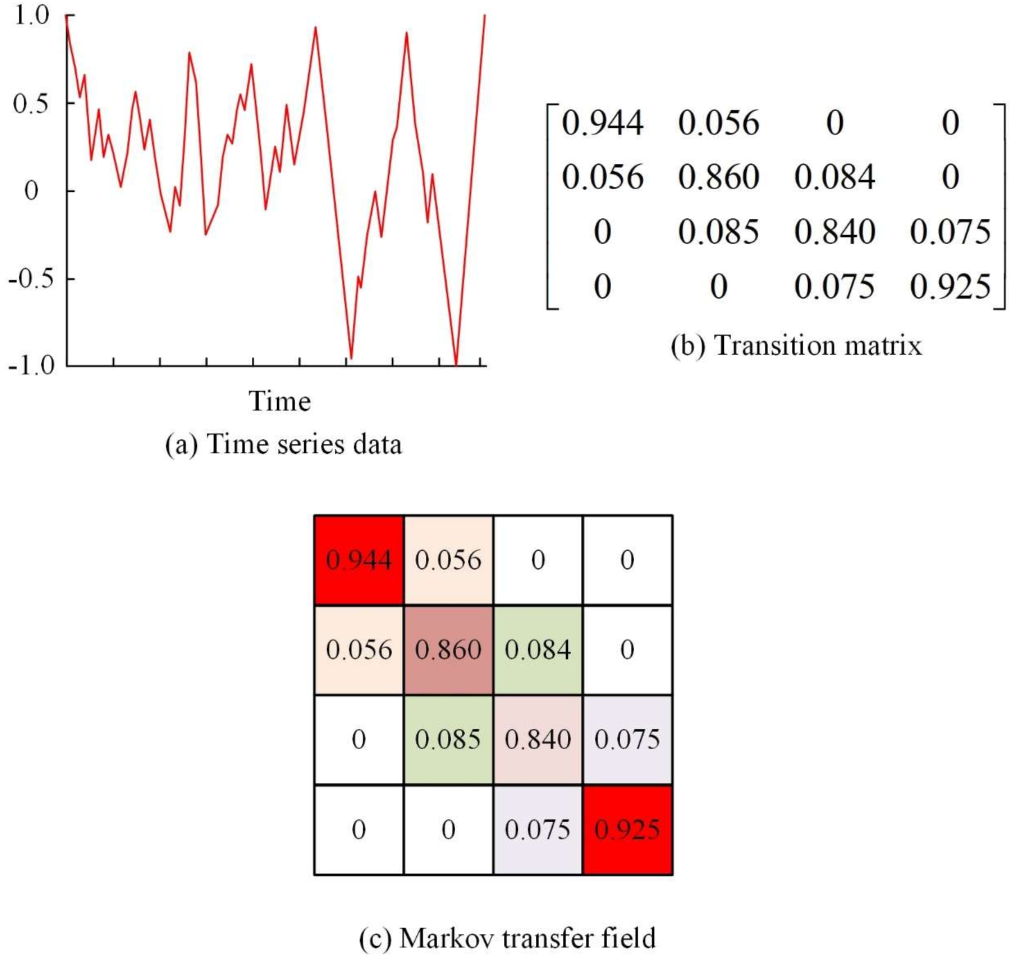

Fig. 3. Markov transfer field diagram

In Figure 3, first, a time series representing human health signals over time is divided into different states. Secondly, by analyzing the discrete states of the time series, the transition matrix between states is established. Next, the transition probability information is visualized as an image. Each pixel of the image corresponds to a transition probability between two states. Finally, MTF images are formed by representing different probability values through color or brightness. The transfer matrix of MTF is shown in formula (5).

$$\rho_l(u, f) = \rho(x_i^l(T+1)) = f \left| x_i^l(T) = u \right. \tag{5}$$

In formula (5), ρ_l is the transition probability. u and f are the state of the image pixels. The transition probability between pixel states is shown in formula (6).

$$m_l(u, f) = E(\rho_l(u, f)) \tag{6}$$

In formula (6), m_l is a two-dimensional image. E is a probability mapping function. The above MTF can effectively capture the transition relationship between time series states, revealing the temporal dependence and potential dynamic patterns in human health signals.

3.4. ECG signal recognition based on DNNAS model architecture

Through the above methods, a signal recognition model based on DNNAS is constructed. This study converts the same ECG signal into the three image expression methods mentioned above, and merges the obtained three images to obtain a more comprehensive feature representation. By integrating three different features, the model may filter out some redundant features, making the final task more focused on information with practical significance. The overall structure of the model is shown in Figure 4.

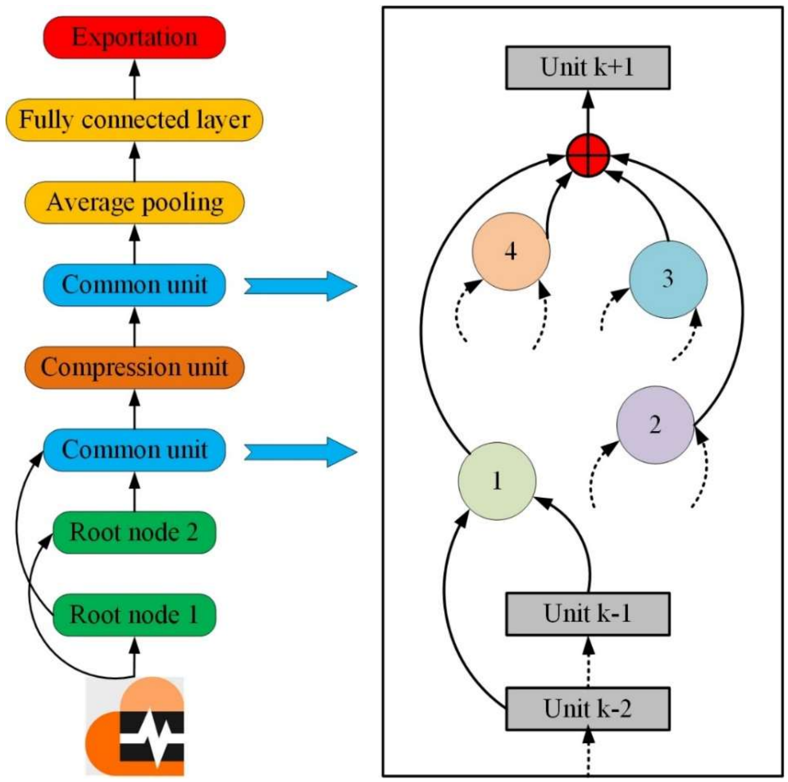

Fig. 4. GCG signal recognition model structure based on DNNAS

In Figure 4, the model design adopts a modular structure specifically designed to process ECG signal features obtained through different image expression forms. The model has two parts, where the main function of the ordinary module is to extract and transform features. The compression module is introduced to effectively reduce the size of feature maps and enhance the receptive field of the model. This module aids the model focus on a larger range of human health data relationships by reducing the size of the feature map. Among them, the discrete operation of nodes is shown in formula (7).

$$B_{i,j}=\sum\frac{\exp\left\{\varepsilon_{i,j}^{o}\right\}}{\sum\exp\left\{\varepsilon_{i,j}^{o'}\right\}}\cdot o(S_{i,j}\cdot a_i)+(1-S_{i,j})\cdot a_i \tag{7}$$

In formula (7), $B_{i,j}$ is the node discrete function, a_i is the output value of the node, o is the candidate operation, ε is the selection weight size, and S is the discrete value. To ensure the fairness of the selection operation, edge normalization is used for processing, as shown in formula (8).

$$a_j=\sum_{i<j}\frac{\exp\left\{\eta_{i,j}\right\}}{\sum_{i<j}\exp\left\{\eta_{i,j}\right\}}\cdot B_{i,j}(a_i) \tag{8}$$

In formula (8), η is the normalized weight of the node output value. This allows the model to focus more on features critical to health management when recognizing EEG signals, improving the efficiency of monitoring and analysis. The structural diagrams of the ordinary module and the Aesop module in the research model are shown in Figure 5.

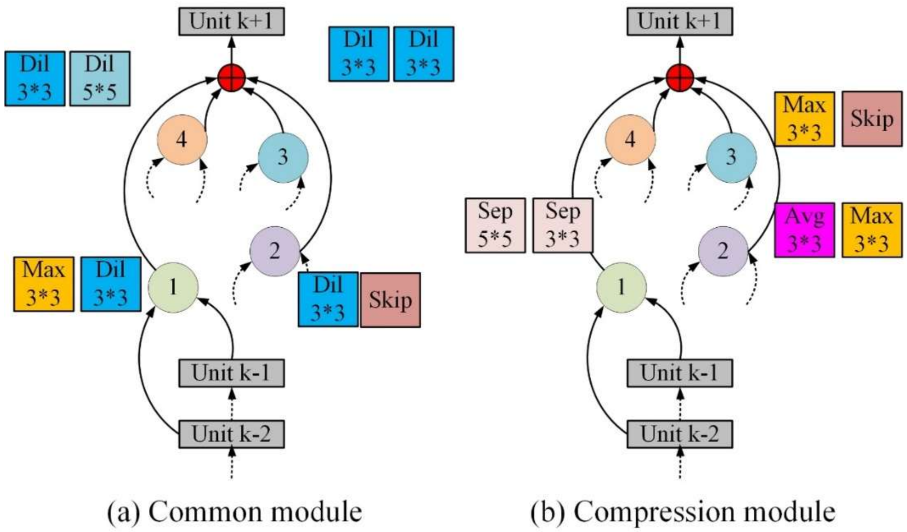

Fig. 5. Module network architecture diagram

In Figure 5, ordinary modules tend to use dilated convolution and compressed convolution. Two convolution operations allow the model to efficiently extract localized features from the input. Extended convolution helps to capture more complex features by increasing the acceptance field. Compressed convolution helps to compress the dimensionality of the features. The compression module tends to choose average pooling and maximum pooling, which help to obtain the overall perspective and global features of the input features.

4. Results

To verify the performance of the proposed method, this study validated the model through experiments. It was analyzed using the PhysioNetMIT-BIH dataset and the PTB diagnostic ECG dataset. The MIT-BIH dataset was created in collaboration between the Massachusetts Institute of Technology and the University of Berkeley, primarily for research on heart disease. This dataset is widely used for heart rate variability analysis, development and evaluation of arrhythmia automatic detection algorithms, containing 48 records with a duration of approximately 30 minutes. Each record is collected from 12 different lead channels. The PTB dataset is provided by the German Heart Center in Berlin, Germany, focusing on the analysis of EEG signals, particularly in the diagnosis of heart diseases. This dataset contains EEG recordings from various heart disease patients, used to evaluate and compare different EEG analysis methods, including 148 EEG recordings from 42 patients. The recording duration is 5 minutes, and the sampling frequency is usually 1kHz. This study divided both datasets into training and testing sets in a 7:3 ratio and validated the models. Table 1 shows the parameter settings of the model in the experiment.

Table 1. Model parameter setting table

Argument	Value	Argument	Value
Batch size	16	Learning rate	0.001
Drop probability	0.35	Weight attenuation	0.001
Initial number of channels	8	Training times	200
Module stack number	5	Momentum	0.99

According to Table 1, the model parameters are set. This study validates the model using both the training and testing sets, and compares and analyzes the Traditional Neural Network (TNN) with the edge detection Canny algorithm. The experiment first uses the training set to verify the accuracy and recall of the model, as shown in Figure 6.

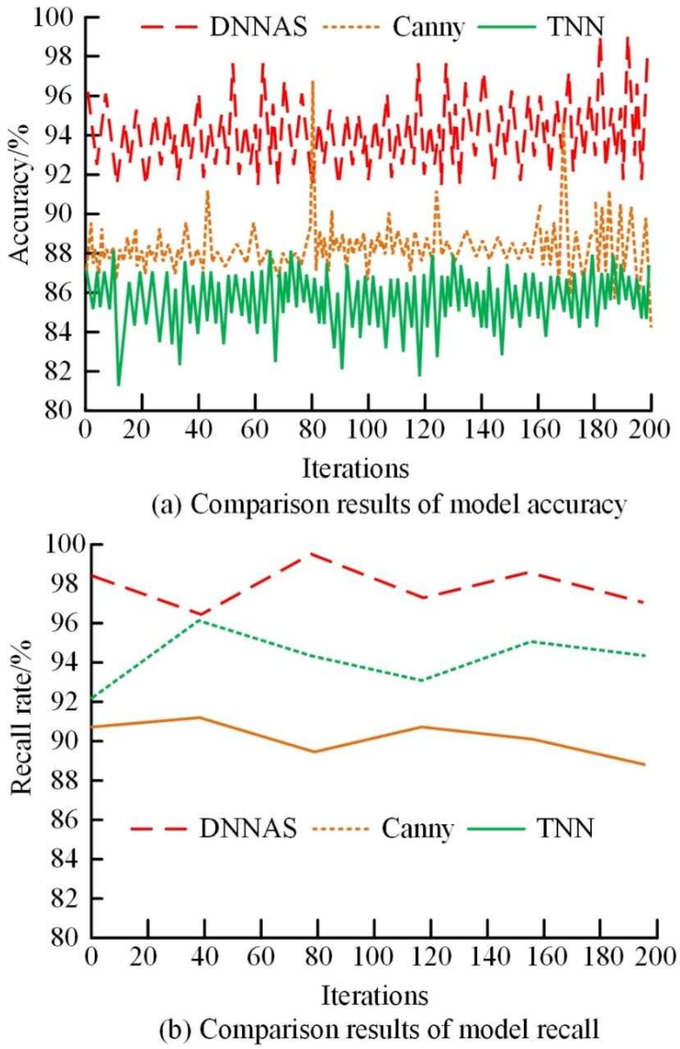

Fig. 6. Results of model accuracy and recall rate

Figure 6 (a) shows the accuracy of the model. The highest accuracy of the research method is 98.5%, with an average accuracy of around 94.0%. The highest accuracy of the Canny algorithm is around 97.0%, with an average accuracy of only 88.0%. The average accuracy of TNN is 7.5% lower than that of the research algorithm. Figure 6 (b) shows the recall rate of the model. The average recall rate of the research algorithm is 98.4%, which is 4.7% and 8.2% higher than Canny and TNN algorithms, respectively. This indicates that research algorithms have better processing capabilities in ECG signal recognition, which is more conducive to the management of human health. The F1 and AUC values of the model for ECG signal detection are shown in Figure 7.

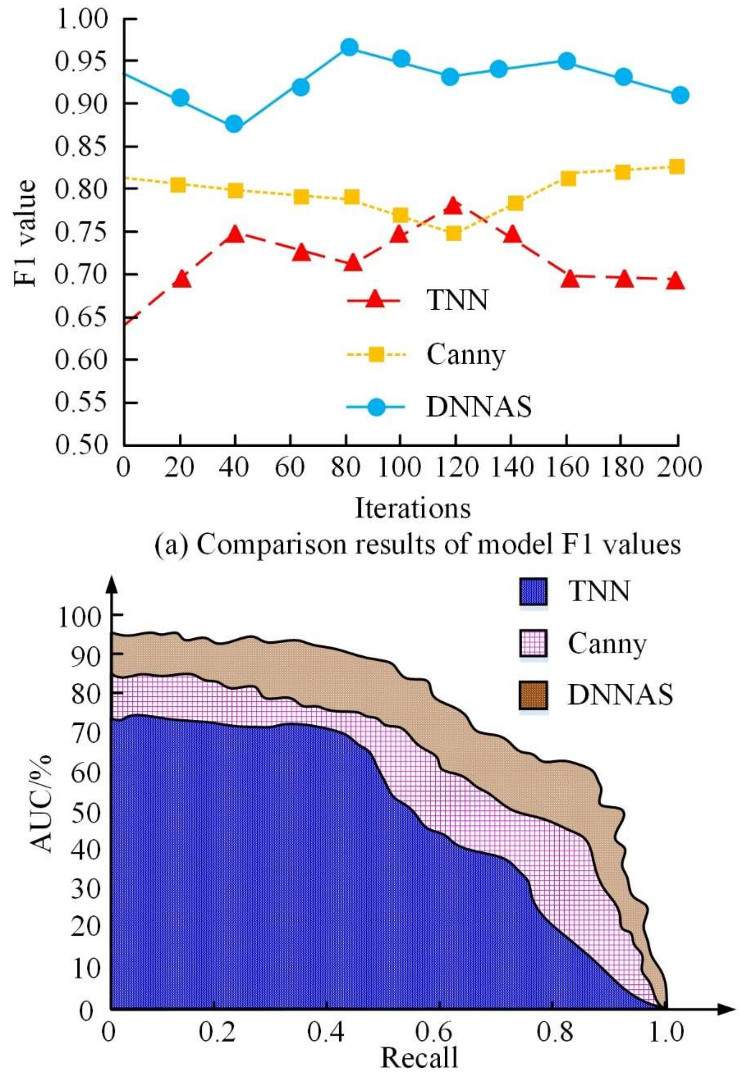

Fig. 7. Comparison of model F1 values with AUC results

Figure 7 (a) shows a comparison of the F1 values of the models. The average F1 value of the DNNAS model is 0.932, which is 0.191 and 0.227 higher than Canny and TNN. Figure 7 (b) shows the AUC value of the model. The AUC value of DNNAS is 0.934, while the AUC value of Canny is 0.892, and the AUC value of TNN is 0.853. This indicates that the DNNAS method has certain potential in ECG signal recognition. This algorithm may be more effective in practical applications, better assisting in the diagnosis and monitoring of heart disease, and improving the quality of patient care and health management. This study compares the true values of ECG signal detection with the predicted values of the model, and uses confidence and support as indicators, as shown in Figure 8.

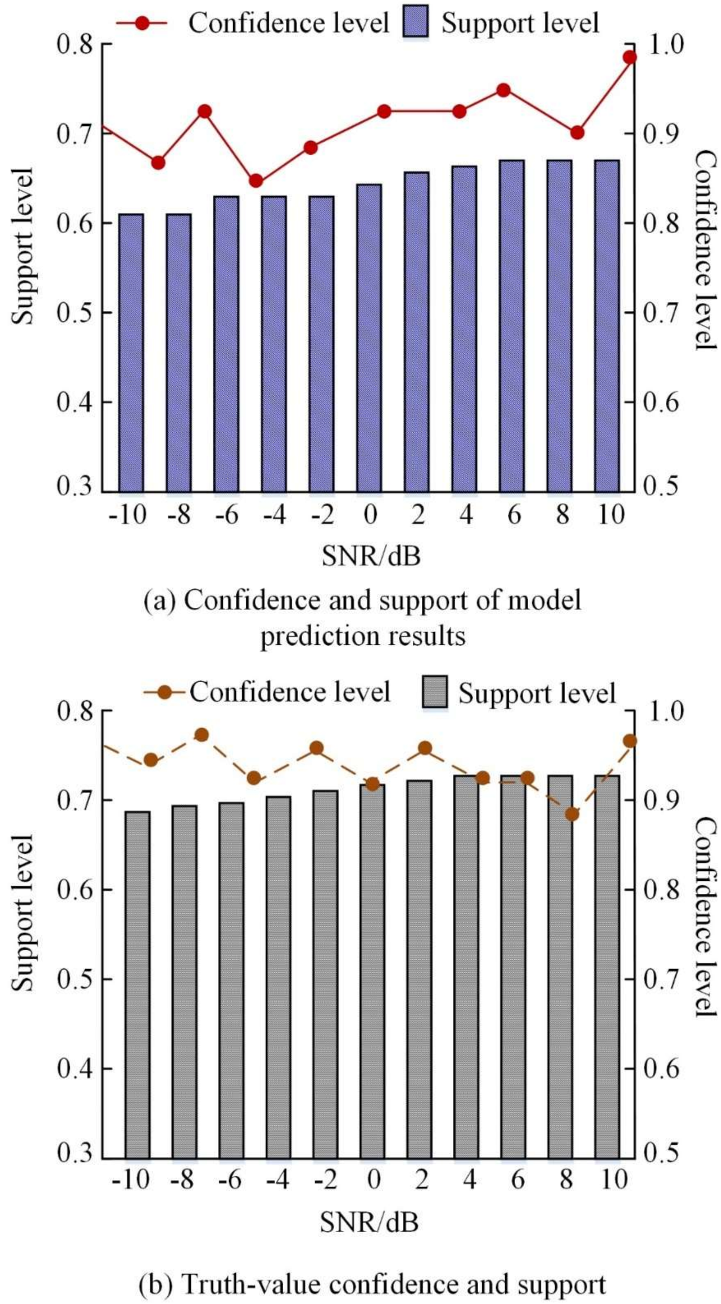

Fig. 8. Comparison results of model confidence and support

Figure 8 (a) compares the confidence and support of the model's predicted values. The average confidence level of the model's prediction is 0.712, and the average support is 0.934. In Figure 8 (b), the confidence level of the true value is 0.718 and the support level is 0.967. The comparison of the predicted values of the research model with the true values has a small error, indicating that the method has a good prediction of human health status. This study trains and tests the model using a training set, and achieves good results. Therefore, the model is further validated using a testing set. In the test set, the loss rate and misidentification rate of the model are shown in Figure 9.

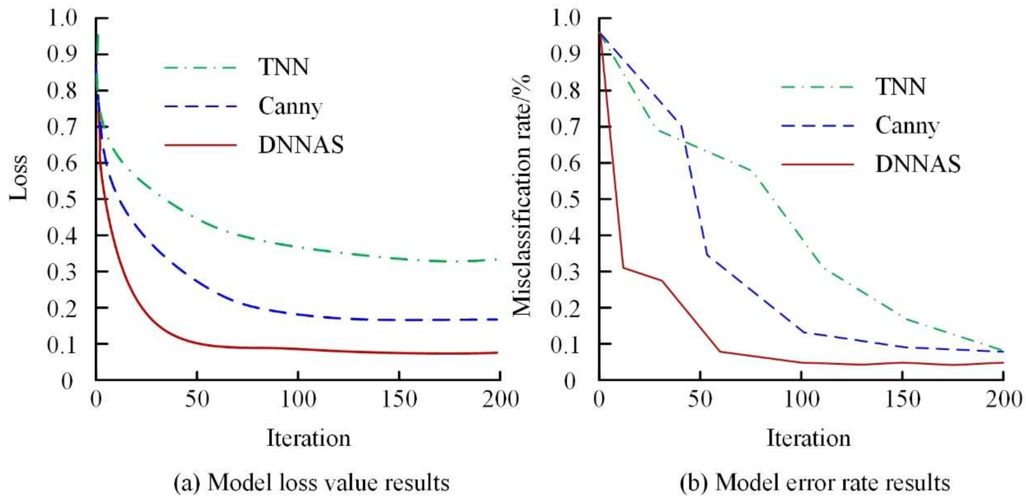

Fig. 9. Results of model loss rate and misidentification rate

Figure 9 (a) shows the model loss rate. At 50 iterations, DNNAS achieved its minimum loss rate of only 0.088, which was 0.103 and 0.226 lower than Canny and TNN, respectively. Figure 9 (b) shows the model misidentification rate. The misidentification rate of DNNAS reached its minimum of 0.052 after 50 iterations. The excellent performance of the DNNAS model in terms of loss rate and misidentification rate indicates that the model has broad prospects for application in EEG analysis. This is important for improving the early diagnosis and management of heart disease, which can improve the accuracy of clinical decision-making and have a positive impact on patient health. This study analyzes the model under different Signal-to-Noise Ratio (SNR) environments, and the prediction accuracy results are shown in Figure 10.

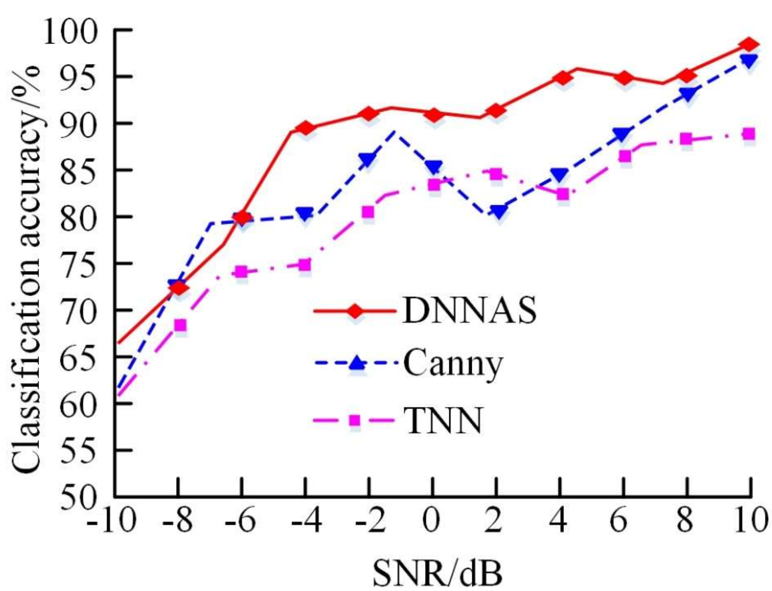

Fig. 10. Prediction accuracy of the model under different SNR environment

In Figure 10, DNNAS has high overall prediction accuracy in different SNR environments. In a 10dB environment, the model's prediction accuracy reaches 98.2%. The prediction accuracy of the Canny model is slightly lower than that of DNNAS, with an accuracy of 95.3%. The prediction accuracy of the TNN model is only 85.6%. Therefore, the research model has reliability in ECG signal recognition. This study compares the validation results of the model on the training and testing sets, as shown in Table

2.

Table 2. Model performance verification analysis

Algorithm	Data set	Sample size	Average accuracy /%
TNN	PhysioNet MIT-BIH	50	78.23
	PTB		79.00
Canny	PhysioNet MIT-BIH		81.57
	PTB		83.89
DNNAS	PhysioNet MIT-BIH		90.32
	PTB		91.49
TNN	PhysioNet MIT-BIH	100	80.34
	PTB		81.11
Canny	PhysioNet MIT-BIH		83.68
	PTB		86.00
DNNAS	PhysioNet MIT-BIH		92.43
	PTB		93.60

In Table 2, among the 50 samples, the average accuracy of DNNAS on the MIT-BIH and PTB datasets is 90.32% and 91.49%, significantly higher than the other two methods. On 100 samples, the performance of DNNAS further improves, with an accuracy of 92.43% in MIT-BIH and 93.60% in PTB. The DNNAS model can achieve high-precision EEG analysis, which helps improve the early diagnosis ability of heart disease. Through effective ECG signal analysis, patients can receive personalized health management recommendations, such as lifestyle adjustments and early intervention. This can help patients better understand their own health status and take corresponding preventive measures.

5. Conclusions

With the increasing incidence of diseases and the growing emphasis on physical health, automated ECG signal analysis is becoming increasingly important. This study proposed a novel ECG signal recognition model based on DNNAS. This model adopted a modular design, which converts ECG signals into various image expressions, fully explores important features in the signals, and combines CNN for deep feature extraction. In the experimental results, the accuracy of the DNNAS model was improved by 4.7% and 8.2% compared to traditional algorithms such as Canny and TNN, respectively. The loss rate of DNNAS was 0.088, which was reduced by 0.103 and 0.226 compared to Canny and TNN. The significant improvement in F1 and AUC values of the model further proved the effectiveness and reliability of DNNAS. The research results reflect the excellent performance of the DNNAS model in ECG signal analysis. This not only helps to quickly identify abnormal ECG activity but also improves the quality of patient care by providing clinicians with a more reliable diagnostic support tool. Although the model performs well, there are still some shortcomings. First, the model does not fully consider the effects of various environmental noises on ECG signals and may have some limitations in practical clinical applications. Future research directions should explore the robustness of models under different noise conditions, evaluate their applicability, and promote the widespread application and development of ECG signal analysis technology.

References

[1] Liu, Y., Wan, C., & Xi, X. (2023). Measurement properties of the EQ-5D-5L in sub-health: evidence based on primary health care workers in China. Health and quality of life outcomes, 21(1), 22.

[2] Shin, J. K. (2016). The study on the relevance of life management and sub-health. Journal of the Korean Data and Information Science Society, 27(4), 925-934.

[3] Luo, S. N., Chen, Y. C., & Kang, T. (2022). Research on Developing Healthy Self-Management Game to Improve College Students' Sub-Health. In Knowledge Innovation on Design and Culture: Proceedings of the 3rd IEEE International Conference on Knowledge Innovation and Invention 2020 (IEEE ICKII 2020) (pp. 267-270).

[4] XUE, Y., XU, J., LIU, G., HUANG, C., FENG, Y., XU, M., ... & CHEN, X. (2021). Evaluation of sub-health status of Chinese Urban residents using the sub-health measurement scale version 1.0. Chinese General Practice, 24(7), 834.

[5] Mahara, G., Liang, J., Zhang, Z., Ge, Q., & Zhang, J. (2021). Associated factors of suboptimal health status among adolescents in China: a cross-sectional study. Journal of multidisciplinary healthcare, 1063-1071.

[6] JIANG, L. J., XU, J., & XIE, J. (2021). Norm of the Sub-health Measurement Scale for the elderly in Tianjin city: an empirical survey. Chinese Journal of Public Health, 37(1), 10-14.

[7] Lu, L., & Chen, Y. (2024). Association Between Suboptimal Health Status and Health-Related Productivity Loss in Primary Healthcare Workers in China: a Cross-Sectional Survey. Risk Management and Healthcare Policy, 1349-1359.

[8] Baek, Y., Jeong, K., Lee, S., Kim, H., Seo, B. N., & Jin, H. J. (2021). Feasibility and effectiveness of assessing subhealth using a mobile health management app (MibyeongBogam) in early middle-aged koreans: randomized controlled trial. JMIR mHealth and uHealth, 9(8), e27455.

[9] Wu, H., Yin, X., Miao, K., Yin, J., & Zhao, H. (2021, January). Cardiorespiratory fitness in adolescents with mental sub-health in China. In Annales Médico-psychologiques, revue psychiatrique (Vol. 179, No. 1, pp. 33-38). Elsevier Masson.

[10] Yang, R., Li, D., Wang, J., Wan, Y., Tao, F., & Zhang, S. (2019). Association of health literacy and physical sub-health among Chinese middle school students. Wei sheng yan jiu= Journal of hygiene research, 48(5), 711-716.

[11] Amoon, M., Altameem, T., & Altameem, A. (2020). Internet of things sensor assisted security and quality analysis for health care data sets using artificial intelligent based heuristic health management system. Measurement, 161, 107861.

[12] Abidi, S. S. R., & Abidi, S. R. (2019, July). Intelligent health data analytics: a convergence of artificial intelligence and big data. In Healthcare management forum (Vol. 32, No. 4, pp. 178-182). Sage CA: Los Angeles, CA: SAGE Publications.

[13] Yang, Y., Siau, K., Xie, W., & Sun, Y. (2022). Smart health: Intelligent healthcare systems in the metaverse, artificial intelligence, and data science era. Journal of Organizational and End User Computing (JOEUC), 34(1), 1-14.

[14] Chen, Z., Qi, H., & Wang, L. (2021, November). Study on the types of elderly intelligent health management technology and the influencing factors of its adoption. In Healthcare (Vol. 9, No. 11, p. 1494). MDPI.

[15] Swamy, T. J., & Murthy, T. N. (2019, January). eSmart: an IoT based intelligent health monitoring and management system for mankind. In 2019 International Conference on Computer Communication and Informatics (ICCCI) (pp. 1-5). IEEE.

[16] Ma, D., Liu, P., & Ge, Z. (2021). Exercise Prescription for the Elderly Based on TCM Physique Characteristics of Sub-healthy Group. Forest Chemicals Review, 1218-1227.

[17] Khan, S., & Yairi, T. (2018). A review on the application of deep learning in system health management. Mechanical Systems and Signal Processing, 107, 241-265.

[18] Balaban, E., Johnson, S. B., & Kochenderfer, M. J. (2019). Unifying system health management and automated decision making. Journal of Artificial Intelligence Research, 65, 487-518.

[19] Vong, J., Song, I., Vong, J., & Song, I. (2015). Automated health care services. Emerging Technologies for Emerging Markets, 89-102.

[20] Muneer, A., & Fati, S. M. (2019). Automated health monitoring system using advanced technology. Journal of Information Technology Research (JITR), 12(3), 104-132.

[21] Beck, B. R., Daly, R. M., Singh, M. A. F., & Taaffe, D. R. (2017). Exercise and Sports Science Australia (ESSA) position statement on exercise prescription for the prevention and management of osteoporosis. Journal of science and medicine in sport, 20(5), 438-445.

[22] Luo, Z., Zhang, T., & Chen, S. (2023). Exercise prescription: pioneering the "third pole" for clinical health management. Research, 6, 0284.

[23] Fruehwirt, W., & Duckworth, P. (2021). Towards better healthcare: What could and should be automated?. Technological Forecasting and Social Change, 172, 120967.

[24] He, C., Li, J., & Vachtsevanos, G. (2015). Prognostics and health management of an automated machining process. Mathematical Problems in Engineering, 2015(1), 651841.

[25] Hong, Y. J., Lee, H., Kim, J., Lee, M., Choi, H. J., Hyeon, T., & Kim, D. H. (2018). Multifunctional wearable system that integrates sweat‐based sensing and vital‐sign monitoring to estimate pre‐/post‐exercise glucose levels. Advanced Functional Materials, 28(47), 1805754.

[26] Li, Q., & Fu, H. Y. (2020). Effects of health management combined with aerobic exercise on cardiopulmonary function in patients with spinal cord injury. International Journal of Clinical and Experimental Medicine, 13(12), 9713-9719.

[27] Zhao, J. (2023). Application effect of health management model in sub-health population. Methods, 5(4), 6-9.

[28] Wu, H., Lin, J., Li, J., Cheng, B., Song, X., Wang, D., & Xu, M. (2020). Modelling and data co-ordination of partial differential equations in sub-health management. Alexandria Engineering Journal, 59(4), 2575-2582.

[29] Sun, J., Li, X., Zhu, Z., & Zeng, J. (2022). An extension method of sub-health intelligent prediction and transformation. Procedia Computer Science, 214, 1554-1560.